

AERODYNAMIC PERFORMANCE OF BLADELESS DUCTED FAN BASED ON EJECTION EFFECT WITH DIFFERENT DESIGN VARIABLES

Kai Han¹, Shilong Yu², Junwei Huang², Junqiang Bai¹, Yasong Qiu¹

- 1. Northwestern Polytechnical University, Unmanned Systems Research Institute, Shaanxi, Xi'an
 - 2. Northwestern Polytechnical University, School of Aeronautics, Shaanxi, Xi'an

Abstract

Based on the development needs for electrification, low noise, and high safety, this research explores the application potential of bladeless ducted propulsion systems (BDPS) based on the ejection effect as a power device for aircraft. The bladeless ducted propulsion system uses a compressor to compress the airflow, which is then ejected at high speed through an annular slit. This high-speed airflow generates low pressure near the inner wall surface, inducing the forward airflow to accelerate backward to obtain thrust. The system mainly comprises an energy device, compressor, air duct, and bladeless ducted propulsion. Firstly, this article provides a brief introduction to the main components of the bladeless ducted propulsion system. Then, based on momentum theory, it analyzes the propulsion characteristics of the bladeless ducted propulsion, deriving theoretical formulas for duct thrust, required power, and propulsion efficiency. It also studies the numerical simulation methods for bladeless ducted propulsion, using the RANS method as a basis to examine the effects of model complexity and grid quantity on propulsion characteristics and the differences between three-dimensional and two-dimensional configurations. Subsequently, the article investigates the impact of several important design variables on the propulsion performance of bladeless ducted propulsion and its flow mechanism. The study finds that design variables such as duct outlet area, inflow speed, and duct length significantly affect thrust characteristics and ejection ratio characteristics. Finally, ground principle flow spectrum tests are conducted to verify the bladeless ducted propulsion, confirming the significant suction effect of the fan.

Keywords: Bladeless Ducted Propulsion system, Momentum theory, numerical simulation methods, design variables

Introduction

The bladeless ducted propulsion system(BDPS) based on the ejection effect is a device that utilizes a compressor to compress the airflow, which is then expelled at high speed through annular slits inside the duct. The high-speed airflow generates low pressure near the inner wall, inducing the forward airflow to accelerate backward to produce thrust. The system mainly consists of a compressor, pipeline, and a bladeless duct.

Compared to traditional ducted fan propulsion system, in terms of appearance, the most striking feature of the bladeless ducted fan is the absence of exposed rotor fan blades and motors, which are replaced by

flexibly arranged compressors. In terms of propulsion principles, traditional ducted fans rely on the rotation of rotor blades to increase the momentum and pressure of the air and move the air backward, and thereby generating thrust. In contrast, in a bladeless ducted propulsion system, the increase the momentum and pressure of the air generated by the compressor does not directly produce force. Instead, it relies on expelling airflow through narrow slits inside the duct, creating low pressure that induces the forward airflow to accelerate backward. This creates a low-pressure area at the lip, thereby generating thrust indirectly. A well-designed bladeless ducted fan can induce a backward massflow up to 15 times its own massflow rate[2].

Thanks to the unique configuration of the bladeless ducted fan, it has three main applications in aircraft:

- 1) as a wing augmentation system to improve the lift-to-drag ratio, delay flow separation at high angles of attack, etc.
 - 2) as a stability and control system.
 - 3) directly as a propulsion device for the aircraft.

In this article, we primarily discuss the third application, as a propulsion device for the aircraft. The main focuses are on the thrust and power characteristics analysis based on momentum theory, the study of numerical simulation methods for the bladeless ducted propulsion system, and the analysis of some conceptual design variables affecting its thrust and power characteristics.

From a theoretical analysis, the bladeless ducted propulsion system has the following characteristics and benefits:

- 1) According to Jetoptera[2], the bladeless ducted propulsion system improves propulsive efficiency by more than 10% while lowering fuel consumption by more than 50% compared to small turbojets. The propulsion system saves approximately 30% in weight compared to turbofans or turboprops and also significantly reduces complexity, which provides significant advantages in the aviation applications.
- 2) The bladeless ducted fan has no exposed fan blades, offering higher safety on the ground and at low altitudes. This prevents safety accidents caused by ground contact with people and avoids power failures caused by bird strikes during low-altitude flight.
- 3) The absence of exposed fan blades also eliminates the noise generated by rotating blades, though it inevitably introduces jet noise at the annular slits. According to Jetoptera[2], an acoustically treated bladeless ducted fan is expected to reduce noise by 25 dB compared to equivalent propellers. Additionally, placing the compressor inside the airframe can further reduce external noise levels.
- 4) The design and placement of the compressor and bladeless ducted fan have a lower degree of coupling. The compressor and bladeless ducted fan can be positioned in their respective optimal working locations. Furthermore, since the bladeless duct is solely responsible for generating thrust and no longer needs to accommodate fixed rotor fan blades, it can deviate from the traditional circular shape and be custom-designed as needed. For example, to increase the lift-enhancing area of a wing, the bladeless ducted fan can be designed in a long, flat shape coupled with the wing.

There has been some research into engineering applications and numerical studies of bladeless ducted propulsion system based on the ejection effect. In terms of engineering applications, Jetoptera[2] [5] has conducted extensive research on their Fluidic Propulsion System (FPS), primarily utilizing bladeless ducted propulsion system based on the ejection effect. They have validated the feasibility of this propulsion scheme

through full-scale wind tunnel models and free-flight tests, and are planning to introduce various models such as the J-220 and J-1000 with different sizes. The United States Navy also adopted an Integrated Lift/Propulsion System (ILPS) based on the ejection effect for the experimental supersonic vertical take-off and landing fighter aircraft XFV-12. Free-flight model tests in full-scale wind tunnels indicated that the aircraft might not achieve vertical take-off solely with its own engine thrust, but the design remained suitable for conventional take-off and landing operations. Vertical take-off and landing trials of the thrust augmentation wing system showed that while the thrust augmentation device did indeed function as expected, the complex and large ducting reduced the effectiveness of engine exhaust flow, decreasing the anticipated wing thrust augmentation from 55% to 19%. In addition to aircraft designs utilizing ejection effect-powered duct, more research has explored applying ejection effects to civilian fans[3] [4], typified by Dyson fans[6]. Overall, bladeless ducted fans based on the ejection effect hold promising application potential in aircraft propulsion systems. However, there remains limited research on the momentum theory derivation and numerical simulation methods specifically for bladeless ducted fan systems.

In terms of numerical and experimental research, Kashif Mehmood et al.[7] employed a method of varying one parameter at a time to study the effects of jet velocity, jet width, fan radius, and fan blade profile angle deviation on aspects such as jet velocity profiles, surface pressure aerodynamics, and other factors for two-dimensional configurations of bladeless fans. Li[8] investigated the impact of parameters including wind channel cross-sectional wing profiles, slit width, cross-sectional height, and slit position on the aerodynamic and noise characteristics of bladeless fans, identifying optimal geometric parameters to guide future designs of bladeless fan configurations. Hong Li[9] conducted research on the flow characteristics, flow field structures, and complete development of jet streams through the exit annular gaps of bladeless fans, elucidating the specific effects of quasi-periodic motion on various stages of jet stream development and intermittent states of turbulent flow fields. Guangxing Zhang[10] used numerical simulation methods to study the influence of curvature and inlet dimensions on the flow field of bladeless fans. Fei Zhao[1] investigated design methods for bladeless fans and internally integrated low-noise fans, assessing the impact of key structural parameters on fan performance and noise indicators. In reference[11], By changing the contraction angle and air outlet gap of the bladeless fan, the main wind area, air supply distance, air volume amplification effect and aerodynamic noise level of the bladeless fan are studied. A comparative analysis is performed with the baseline configuration to find the optimal contraction angle and optimal air outlet gap. Lei Wang[12], focusing on misting fans, conducted orthogonal experiments on factors such as cross-sectional distance, guiding angle, exit angle, and slit width affecting the performance of annular jet mechanisms in wind-driven misting systems, verifying operational performance through experimental tests. The aforementioned studies primarily focus on the characteristics of bladeless fans, aligning with principles underlying bladeless ducted fan technology.

Currently, research on bladeless fans based on the ejection effect has largely focused on fans rather than propulsion devices. There is a lack of scholarly references on representative studies focusing on bladeless ducted fans as propulsion devices. Bladeless ducted propulsion system differ from traditional propulsion systems in system composition and propulsion principles, showing potential applications in specific configurations. Therefore, it is worthwhile to conduct in-depth research on their propulsion performance.

This paper starts with a focus on the propulsion performance of bladeless ducted fans. It begins by studying and elucidating the components of bladeless ducted propulsion system based on ejection effect. The theoretical derivation of propulsion principles is explored from a momentum theory perspective, explaining the relationships among various physical quantities in bladeless ducted propulsion system. Subsequently, critical numerical simulation methods are investigated. Key design variables affecting the performance of bladeless ducted fans are then studied. Based on the research into its thrust characteristics, comparative studies are conducted on important performance data such as propulsion efficiency. A simple demonstration and verification of principles are performed on the ground to demonstrate the suction effect of bladeless ducted fans.

Composition of bladeless ducted propulsion system

A integral bladeless ducted propulsion system consists of four main components: compressor, power source, bladeless duct, and pipelines. The schematic diagram of its operation is shown in Fig. 1.

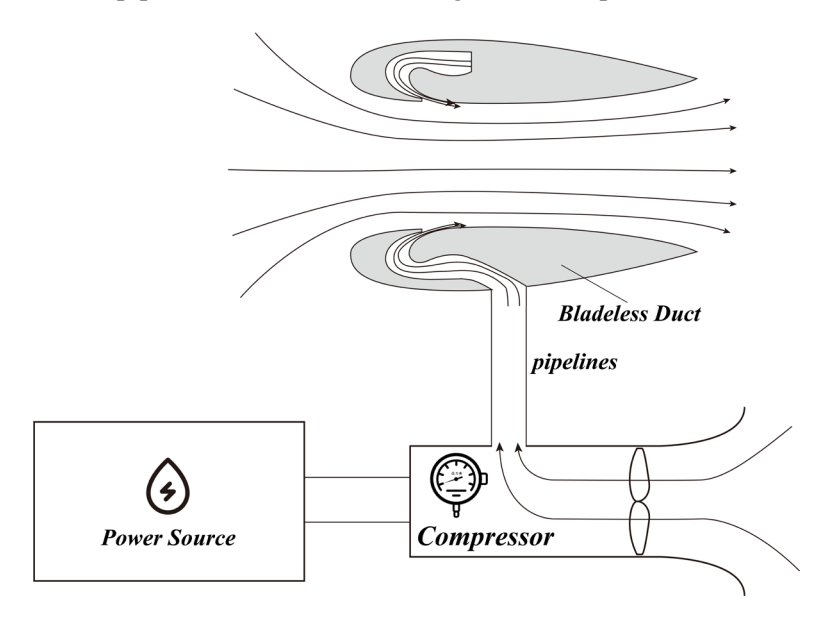


Fig. 1 Composition of bladeless ducted propulsion system

Compressor

In the bladeless ducted propulsion system, a high-efficiency lightweight compressor is one of the key core technologies. The main function of the compressor is to intake external air, compress it, and transfer it through pipelines into the cavity inside the bladeless duct. Factors influencing compressor design parameters mainly include the required thrust, which related with flow characteristics and the back pressure of the cavity.

Power Source

The power source drives the compressor to provide gas for the bladeless duct. The choice of energy form primarily depends on the aircraft's flight mission and the energy density of the power source.

Bladeless Ducted Fan

The bladeless duct is the device that generates thrust. The compressor inputs air through ducting into the cavity of the bladeless duct. The air is then expelled through annular slits on the inner wall of the bladeless

ducted fan, accelerating backward through momentum mixing and induced low pressure. A larger frontal flow capture area induces low pressure at the lip of the duct, generating thrust. Since the bladeless ducted fan no longer has circular fan blades inside, the shape of the bladeless ducted fan has higher design flexibility. Jetoptera has developed some bladeless ducted fans with rounded rectangular shapes.

Pipelines

pipelines connects the compressor and the bladeless duct, transferring gas to the bladeless duct. The presence of pipelines allows for decoupled design and placement of the compressor and the bladeless duct, which increasing aerodynamic design flexibility.

Performance Analysis of Bladeless Duct Based on Momentum Theory

Thrust Characteristics Analysis of Ducted Fans Based on Momentum Theory

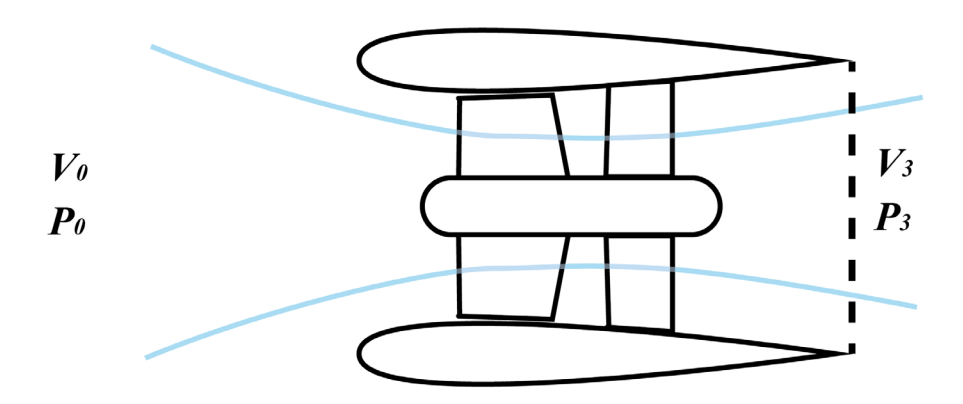


Fig. 2 Simplified Principles of Momentum Theory for Ducted Fans

In the momentum theory analysis of traditional ducted fans, the thrust of all components can be calculated using the following formula:

$$T = \dot{m}_3 (V_3 - V_0) + (P_3 - P_0) A_3 \tag{1}$$

In the above equation, V_0 represents the free-stream velocity, V_3 is the velocity at the duct exit, P_0 is the free-stream static pressure, P_3 is the static pressure at the duct exit, and \dot{m}_3 represents the mass flow rate passing through the duct.

The energy changes in two aspects after the airflow is transformed from free flow to pass through the rotating blades,. The motor shaft power mainly changes into the increase of airflow kinetic energy and the increase of enthalpy. The power expression for calculating the increase of kinetic energy is as follows:

$$P_{V} = \frac{1}{2}\dot{m}\left(V_{3}^{2} - V_{0}^{2}\right) \tag{2}$$

The expression for the power required for the increase in enthalpy is:

$$P_H = c_p \dot{m} \left(T_3 - T_0 \right) \tag{3}$$

In the above expression, c_p is the specific heat capacity at constant pressure.

Therefore, the expression for calculating shaft power using momentum theory is:

$$P = P_H + P_V \tag{4}$$

Therefore, the propulsion efficiency of the ducted fan can be calculated using the following expression:

$$\eta = \frac{\left(\dot{m}_3 \left(V_3 - V_0\right) + \left(P_3 - P_0\right) A_3\right) \cdot V_0}{\frac{1}{2} \dot{m}_3 \left(V_3^2 - V_0^2\right) + c_p \dot{m}_3 \left(T_3 - T_0\right)}$$
(5)

verification of thrust characteristics of ducted fans based on momentum theory

This section takes a ducted fan as an example to verifying the accuracy of momentum theory calculations. The ducted fan has 10 rotor blades and 8 stator blades, with the rotor blades in front and the stator blades in the back. Verify the accuracy of the momentum theory method proposed in previous section to solve the thrust and power characteristics.

In order to reduce the amount of calculation, the ducted fan is evaluated using a single-channel configuration, that is, a single rotor blade and a single stator blade are evaluated, and a block grid generation strategy is adopted, that is, grids are generated according to the three domains of duct and far field, rotor blades and stator blades, and then merged according to their relative positions, and interface boundary conditions are applied between different domains for flux transfer. Periodic rotation boundary conditions are applied on both sides of the far field domain, rotor blade domain, and the stator blade domain to simulate the effect of a full-channel ducted fan. In the far field domain, the far field domain length of the grid in front of the fan is about 160 times the diameter of the fan, the far field domain length of the grid behind the fan is about 240 times the diameter of the fan, and the far field radial grid scale is about 120 times the diameter of the fan. The model diagram and boundary condition diagram are shown in Fig. 3.

The ducted fan calculation conditions are shown in Table 1.

Table 1 ducted fan calculation conditions

Property	Number	
Freestream velocity	30m/s	
Diameter of inner surface of duct	223.318mm	
RPM of fan	7000RPM	
Number of rotor blades	10	
Number of stator blades	8	

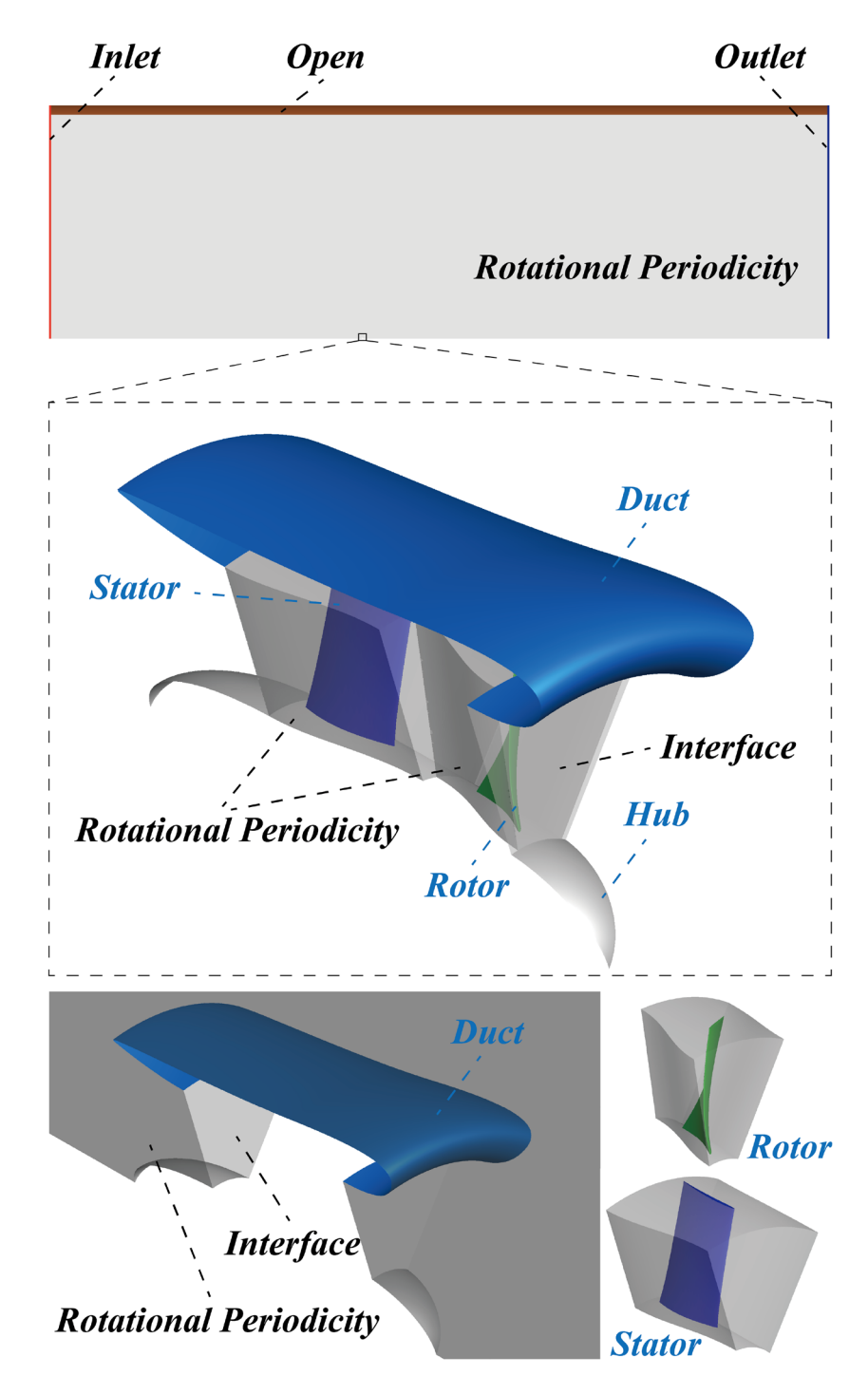


Fig. 3 Ducted fan calculation domains and boundary condition settings

Based on the above momentum theory, the thrust and power of the ducted fan mentioned above are computed and compared with the RANS calculation results as shown in Fig. 4. In general, the calculation results based on momentum theory are consistent with the results of the RANS method. In terms of thrust calculation, the value calculated by momentum theory is larger than the result of RANS method. Within the research range, the absolute error of thrust calculated by the two methods is less than 1N, and the reasoning error tends to decrease with the increase of rotation speed. In terms of power, the result obtained by

momentum theory is smaller than that of the RANS method, and the absolute error of power calculation increases with the increase of rotation speed. Within the research range, the absolute error is less than 30W. The result of propulsion efficiency calculated based on momentum theory is larger due to the larger thrust and smaller power, and the absolute error of propulsion efficiency gradually decreases with the increase of rotation speed.

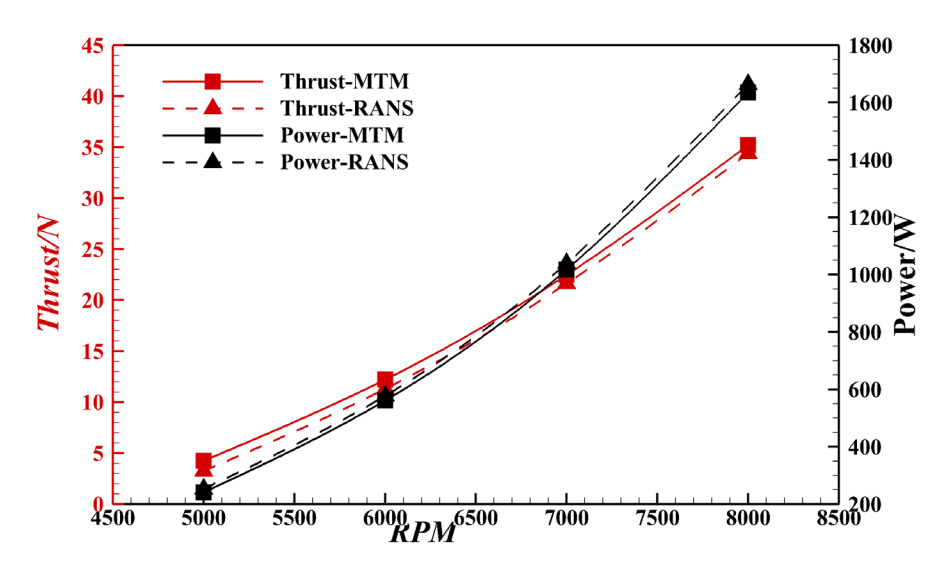


Fig. 4 Comparison of thrust and power calculation results of ducted fan using momentum theory and RANS method

Analysis of thrust and power characteristics of bladeless duct based on momentum theory

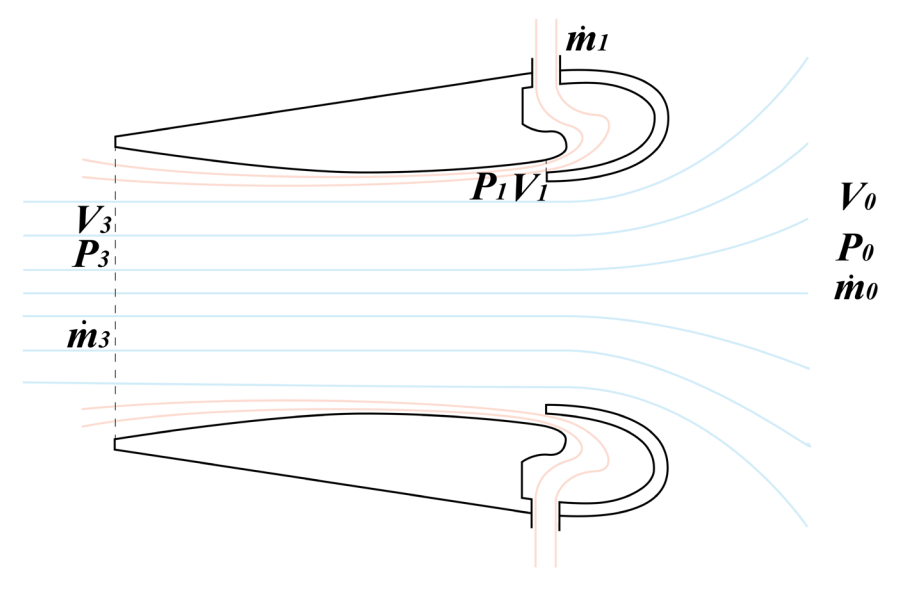


Fig. 5 Principle Momentum Theory Model of Bladeless Duct

Based on the introduction and verification of the momentum theory of the ducted fan in the previous section. Assuming that the mass flow rate provided by the compressor for the bladeless power duct is \dot{m}_1 , the jet slit area is B_2 , the air density is ρ , and assuming that the air flow velocity ejected from the slit is uniform, the jet velocity at the slit is

$$V_2 = \frac{\dot{m}_1}{\rho B_1} \tag{6}$$

The ejection ratio c is defined as the ratio of the mass flow increment induced backward to the mass flow of the jet in the slit. As shown in expression (2), the ejection ratio is related to the design parameters of the bladeless duct, such as the gap width and the duct outlet area.

$$c = \frac{\Delta \dot{m}_4}{\dot{m}_1} \tag{7}$$

In the above formula, $\Delta \dot{m}_4$ is the mas flow increment entering the duct due to the induction effect, and the calculation formula of is:

$$\Delta \dot{m}_4 = \dot{m}_3 - \dot{m}_4 \tag{8}$$

In the above formula, \dot{m}_3 is the actual mass flow rate through the duct under the induction effect, \dot{m}_4 is the mass flow rate of the airflow through the duct without the jet induction effect. Assuming that the duct outlet area is A_3 , the velocity at the outlet is:

$$V_3 = \frac{\dot{m}_3}{\rho A_3} \tag{9}$$

The thrust of the bladeless duct is:

$$T = \dot{m}_3 V_3 - \dot{m}_0 V_0 + (P_3 - P_0) A_3 \tag{10}$$

In the above formula, V_{θ} is the free flow velocity, P_{θ} is the free flow static pressure, and \dot{m}_2 is the mass flow rate in the duct without jet mixing, that is, it satisfies the following equation:

$$\dot{m}_3 = \dot{m}_0 + \dot{m}_1 \tag{11}$$

There are two methods to solve the power of bladeless duct, which are analysis from the duct perspective and compressor perspective:

Analyzing from the duct perspective, after the airflow is ejected from the annular slit, it brings three changes to the airflow in the duct, namely, the change of airflow velocity, the change of airflow pressure and the change of airflow temperature. That is, the first item corresponds to the change of kinetic energy, and the last two items correspond to the change of enthalpy.

Taking the bladeless duct system as the research object, the free flow velocity is V_0 , the jet velocity is V_2 , and the velocity at the duct outlet is V_3 . Since the velocity V_3 at the duct outlet is not uniform along the radial direction, the outlet velocity V_3 averaged by the mass flow rate is used in the actual calculation. Then the power of kinetic energy change is:

$$P_{V1} = \frac{1}{2}\dot{m}_3 V_3^2 - \frac{1}{2}\dot{m}_0 V_0^2 - \frac{1}{2}\dot{m}_1 V_1^2$$
 (12)

The power required for the enthalpy change of the air flow is:

$$P_{H1} = c_p T_3 \dot{m}_3 - c_p T_1 \dot{m}_1 - c_p T_0 \dot{m}_0 \tag{13}$$

In the above formula, T_0 is the air flow temperature of the free flow, T_I is the air flow temperature at the jet outlet, T_3 is the air flow temperature at the duct outlet, and c_p is the specific constant pressure heat

capacity.

Therefore, from the perspective of bladeless duct, the power required to generate thrust T is:

$$P_1 = P_{V1} + P_{H1} \tag{14}$$

From the above formula, we can know that the propulsion efficiency of the bladeless duct is:

$$\eta = \frac{TV_0}{P_1} = \frac{((\dot{m}_3 V_3 - \dot{m}_2 V_0 + (P_3 - P_0) A_3) \cdot V_0)}{\frac{1}{2} \dot{m}_3 V_3^2 - \frac{1}{2} \dot{m}_0 V_0^2 - \frac{1}{2} \dot{m}_1 V_1^2 + c_p T_3 \dot{m}_3 - c_p T_1 \dot{m}_1 - c_p T_0 \dot{m}_0}$$
(15)

In the whole system, the duct component only generates thrust, so the power can also be analyzed from the perspective of the compressor.

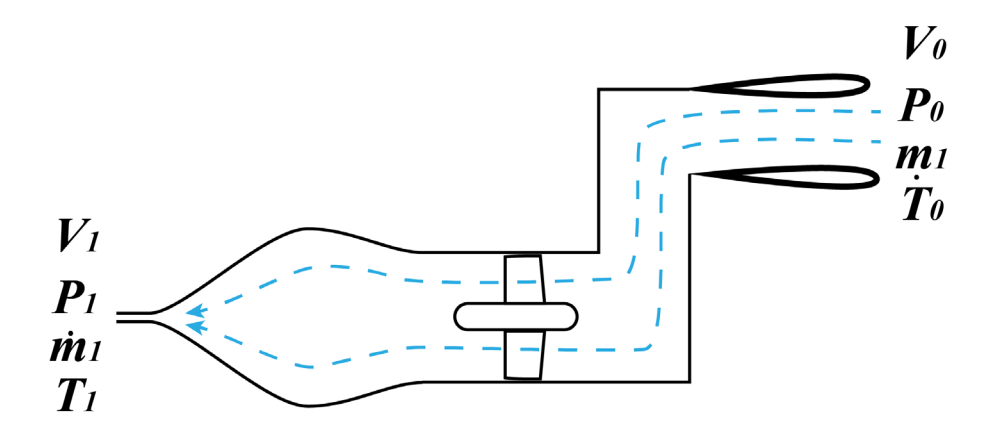


Fig. 6 Simplified schematic model of the compressor and flow path

In Δt , the air is pressurized from the free flow state and then transported through the pipeline. In the pipeline, the cross-sectional area of the airflow will change irregularly. When the airflow is ejected from the annular slit, the power done by the compressor can cause two changes, the change in kinetic energy and the change in enthalpy. The power required for the change in kinetic energy can be expressed as:

$$P_{V2} = \frac{1}{2}\dot{m}_1 V_1^2 - \frac{1}{2}\dot{m}_1 V_0^2 \tag{16}$$

In the above formula, V_I is the annular slit jet velocity, and V_0 is the compressor inlet air velocity. Since the compressor also inhales gas from the freestream, it is assumed that its inlet air velocity is the same as the free flow velocity.

The power required for the change in enthalpy can be expressed as:

$$P_{H2} = hT_1\dot{m}_1 - hT_0\dot{m}_1 \tag{17}$$

Therefore, from the perspective of the compressor, the power required for the bladeless duct is:

$$P_{2} = P_{V2} + P_{H2} = \frac{1}{2}\dot{m}_{1}V_{1}^{2} - \frac{1}{2}\dot{m}_{1}V_{0}^{2} + c_{p}T_{1}\dot{m}_{1} - c_{p}T_{0}\dot{m}_{1}$$
(18)

From the above formula, we can know that the propulsion efficiency of the bladeless duct is:

$$\eta = \frac{TV_0}{P_2} = \frac{(\dot{m}_3 V_3 - \dot{m}_0 V_0 + (P_3 - P_0) A_3) \cdot V_0}{\frac{1}{2} \dot{m}_1 V_1^2 - \frac{1}{2} \dot{m}_1 V_0^2 + c_p T_1 \dot{m}_1 - c_p T_0 \dot{m}_1}$$
(19)

Without considering the flow loss inside the gas pipeline, the power calculated by the two methods is theoretically the same, namely:

$$P_1 = P_2 \tag{20}$$

Numerical simulation methods

In this study, a high-precision solution method based on the Reynolds-averaged NS (RANS) equations was applied using the k- ω SST turbulence model.

Study on the complexity of duct model

There is almost no literature that systematically studies the numerical simulation methods of bladeless duct. In this section, we compare the numerical simulation methods for three three-dimensional configurations from simple to complex, in order to find an accurate and simple numerical simulation method. Since the research object of this research is the bladeless duct, the thrust characteristics of the bladeless duct are mainly focused on, and the performance of the compressor and the gas pipeline are not concerned.

The thrust of the bladeless duct mainly relies on the low-pressure area generated by the high-speed jet to induce the front airflow to accelerate backward. Therefore, relative to the jet-free state, the most critical thing is the simulation of the jet.

In these three configurations, the basic duct surface size and shape are the same, and the jet flow rate is also the same. Configuration A directly applies the velocity inlet boundary condition on the virtual surface at the annular jet outlet close to the inner wall, without considering the internal cavity, and only considering the influence of the jet on the external surface. Configuration B takes the internal cavity into consideration, but does not consider how the airflow comes in. It only applies the velocity inflow boundary condition at the blue circle in the following figure (b), so that it flows along a cavity with a gradually decreasing cross-sectional area and a bend in the flow direction, and finally flows out through the jet slit near the inner wall. Although this configuration takes the internal flow channel into consideration, the way the gas flows in is far from the truth. Configuration C considers how the airflow enters the cavity, that is, connecting the outside and the cavity through four cylindrical pipes, without considering the connection between the exposed cylindrical pipes and the compressor. The flow velocity inlet boundary condition is applied at the four cylindrical pipes. This configuration is closer to reality.

The simulation degree of configuration A, configuration B, and configuration C is getting closer to the real situation. In order to study the thrust generated by different components in the bladeless duct, configuration A is divided into two parts, namely the lip with the outer wall surface and the inner wall surface, as shown in Fig. 8 for configuration A; configurations B and C are divided into three parts, namely the lip with the outer wall surface, the inner wall surface and the inner flow channel.

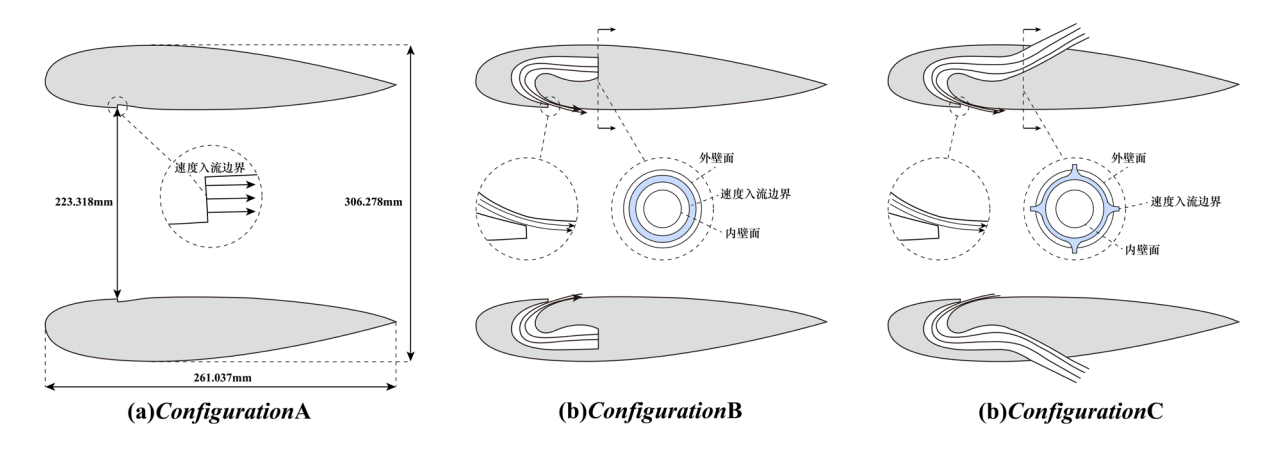


Fig. 7 Two-dimensional cross-sectional views of the object of study at three different levels of simplification.

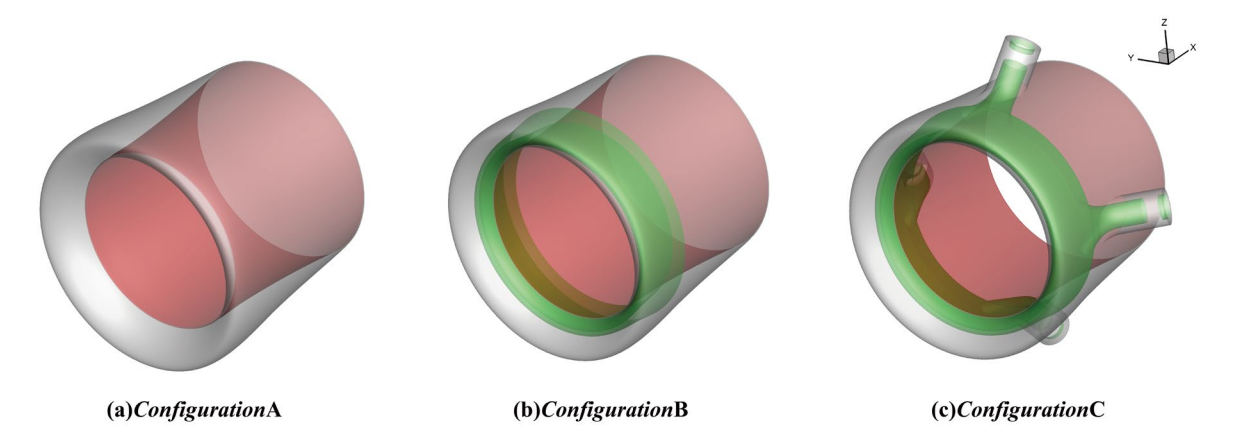


Fig. 8 Schematic diagram of the component division of the research object with three different simplification levels

Table 2 shows the fan thrust data obtained using the surface force integration method (positive value is positive thrust, negative value is negative thrust), and its operating conditions and model dimensions are shown in Table 3:

As shown in Table 2, the thrust obtained by using the surface force integration to calculate the three configurations with the same configuration and the same jet flow rate is very different. The main difference is caused by the surface integral of the high pressure inside the inner flow channel in the flow direction. As shown in Figure 6, since configuration A has no inner flow channel, its thrust is negative. The same configuration uses numerical simulation methods with different degrees of simplification to obtain very different calculation results, so it is not certain which calculation method should be used.

Table 2 Force division results of components of different configurations

Configuration	Thrust of lip with the outer wall surface[N]	Thrust of in- ner wall [N]	Thrust of inner flow channel [N]	All thrust[N]
A	-1.091	-9.187		-10.28
В	-0.3056	-7.692	620.1	612.10
С	-3.2	-8.037	107.142	95.905

Table 3 Bladeless duct operation conditions		
Property	Number	
Free stream velocity	30m/s	
Jet mass flow	0.1kg/s	
Diameter of inner duct	223.318mm	
Height of flight	0km	
Cp: -1 -0.9-0.8-0.7-0.6-0.5-0.4-0.3-0.2-0.1	0 0.1 0.2 0.3 0.4 0.5 0.6 0.7 0.8 0.9 1	

(b)ConfigurationB Fig. 9 Pressure coefficients of three different simplified configuration sections

(a)ConfigurationA

(b)ConfigurationC

Based on the momentum theory method in previous section, the thrust and power characteristics of the three configurations are evaluated. The results are shown in Table 4. Taking the most complex configuration C as the benchmark, in terms of thrust, the calculation relative error of configuration A is 4.02%, and the relative error of configuration B is 6.27%. In terms of power, the relative error of configuration A is 0.85%, and the relative error of configuration B is 4.72%. In terms of propulsion efficiency, the relative error of configuration A is 2.37%, and the relative error of configuration B is 0.86%. In terms of ejection ratio, the relative errors of configuration A and configuration B are both around 9.6%. In terms of thrust characteristics, both configuration A and configuration B can meet the basic requirements of the evaluation.

In terms of thrust calculation, the same configuration with the same jet flow rate input and the use of RANS-based numerical simulation methods with different degrees of simplification should theoretically obtain similar calculation results. When the surface force integral method is used to calculate thrust, the thrust calculation results are very different due to the different internal cavity structures, while the calculation method based on momentum theory can obtain similar thrust calculation results. Due to the lack of effective methods for measuring bladeless power duct thrust, according to theoretical analysis, the degree of trust in the momentum theory calculation results in this article is much greater than that based on the surface force integral method, and the subsequent results will only show the thrust calculation characteristics based on momentum theory.

Table 4 Thrust characteristics and ejection ratio characteristics of different configurations

Configuration	Thrust[N]	Power[W]	Propulsion efficiency	ejection ratio
A	14.874	991.770	0.45	3.113
В	14.525	953.047	0.457	3.109
C	15.497	1000.246	0.465	3.4412

Table 5 compares the grids amounts and the calculation time of the three configurations. All three configurations generate structured meshes with similar density and are calculated using the same solver on the same high performance computer.

Combining the comprehensive evaluation of calculation accuracy and calculation time, in the subsequent evaluation, configuration A is used as the research object to study the influence of different design variables on its aerodynamic performance.

Table 5 Comparison of different configurations of grid amounts and calculation time

Configuration	Grids amounts	calculation time [h]
A	1598592	11.6
В	2315064	16.8
C	9174356	84

Verification of Grid Independence

Taking configuration A as the research object, the influence of four grid amounts on the performance of bladeless duct propulsion are studied. The grid amounts are approximately 800,000, 1.6 million, 3.2 million, and 4.8 million, respectively. The thrust and power characteristics are shown in Fig. 10. The thrust characteristics and power characteristics change curves become flat at 3.2 million grid amounts. Therefore, in order to balance the relationship between the increase in calculation time and calculation accuracy caused by the increase in grid amounts, the 3.2 million grid amounts is studied subsequent research.

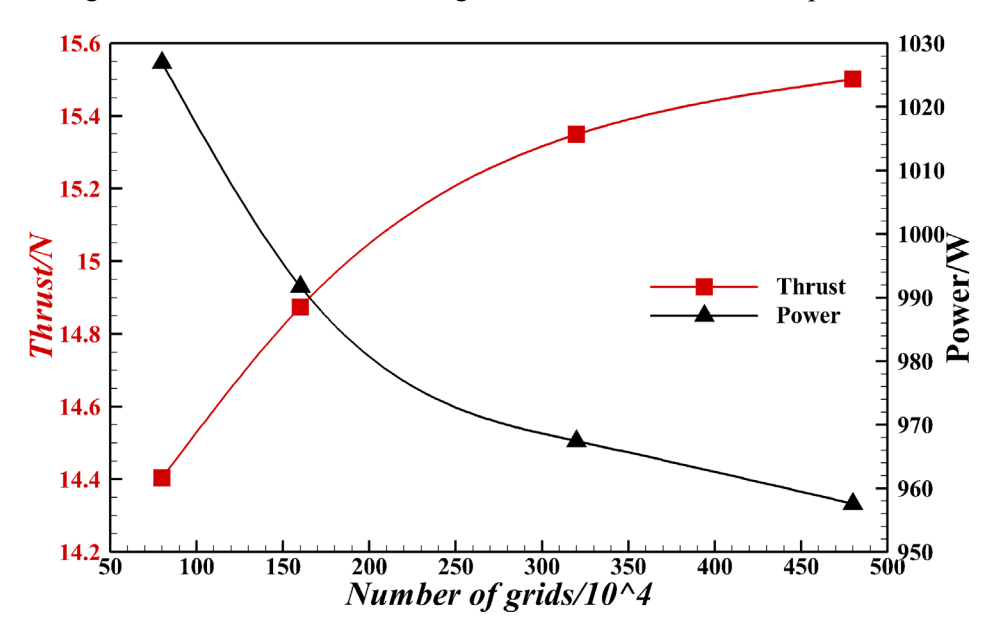


Fig. 10 Thrust and power performance trends with grid volume

Comparison of 3D and 2D impact

Compared with the three-dimensional configuration studied in the previous research, the grid amounts of the two-dimensional configuration under similar grid density can be reduced to 96700, due to the limitation of the solver, the two-dimensional grid described in this article is actually a thin space constructed by two layers of grids. According to the flow rate per unit area, a new variable can be defined, that is, the mass

flow surface density, which is the following formula, where \dot{m} is the jet flow rate, A is the jet outlet area, and the mass flow surface density of the three-dimensional configuration is kept consistent with that of the two-dimensional configuration. Based on the above numerical simulation method, it is numerically calculated to obtain the flow field comparison shown in Fig. 11.

$$\ddot{m} = \frac{\dot{m}}{A} \tag{21}$$

It can be seen from the figure that the air flow velocity in the duct of the three-dimensional configuration is higher than that of the two-dimensional configuration, that is, the ejection effect of the three-dimensional configuration is greater than that of the two-dimensional configuration. A similar flow field cannot be obtained under the same mass flow surface density. This is mainly due to the configuration characteristics of the two-dimensional configuration. Its ejection is limited to the two-dimensional plane rather than in the three-dimensional space, which hinders the ejection effect.

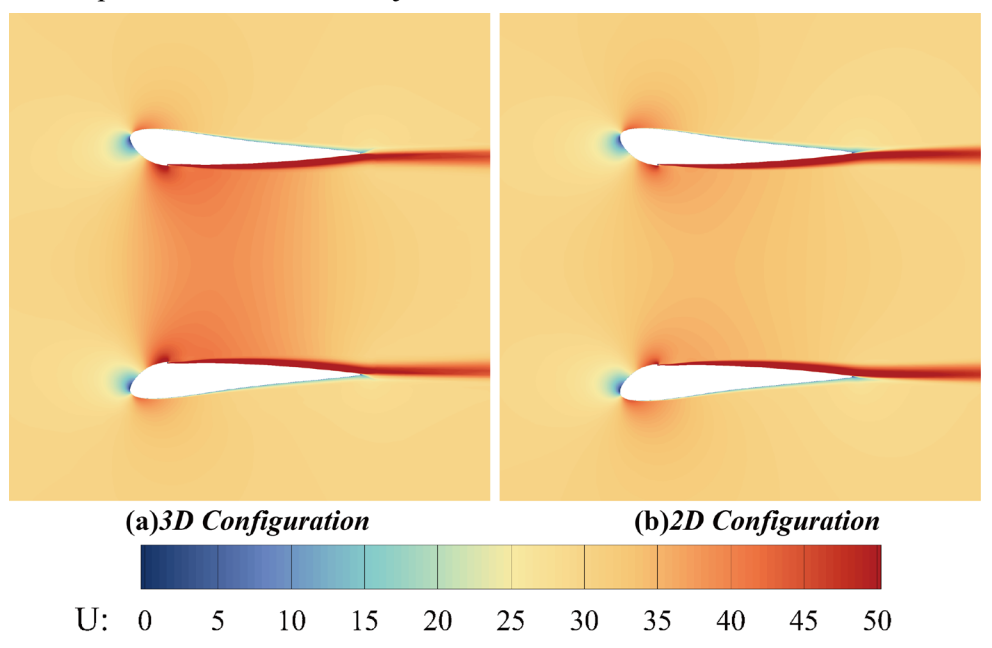


Fig. 11 Comparison of flow fields between two-dimensional and three-dimensional cross-sections

Influence of Design Variables on Bladeless Power Duct

Bladeless duct outlet area

Similar to traditional ducted fans, changing the duct outlet area can change the flow capacity of the airflow, and thus change the thrust characteristics of the ducted fan. In a bladeless duct, the same jet flow rate is input, and the ejection effect and thrust characteristics will also have different performances under different duct outlet areas.

In the configuration A, the duct outlet has a slight expansion trend. In this section, taking configuration A as the baseline (i.e., Design 2 in Table 6), the outlet area is changed to obtain different configurations, as shown in Fig. 12. The operating conditions of the five configurations are shown in Table 3. As shown in Table 6, In terms of thrust characteristics, the larger the area, the smaller the thrust, and for the ejection ratio, it increases monotonically with the increase of the duct outlet area within the research range.

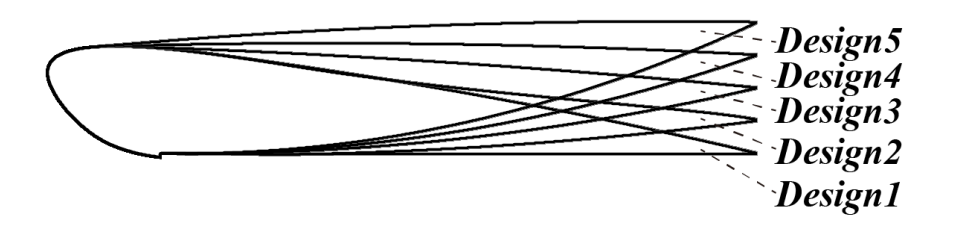


Fig. 12 Comparison of different duct outlet area designs

Table 6 Thrust characteristics and ejection ratio characteristics of different designs

Table of thrust characteristics and ejection ratio characteristics of uniform designs		
Configuration	Thrust[N]	Ejection ratio
Design1	14.999	1.777
Design2	14.874	3.113
Design3	13.831	5.579
Design4	13.12	10.038
Design5	9.162	15.685

Free stream velocity

This section studies the effect of the incoming flow velocity on the thrust characteristics based on Configuration 2 in previous section. Similar to traditional ducted fans, as the incoming flow velocity increases, the stagnation point of the duct lip gradually moves downward, the thrust generated by the duct lip becomes smaller, and the fan's ejection ratio also becomes smaller.

Table 7 Thrust and ejection ratio characteristics at different free stream velocities

Tubic / Timust and	Tuble 7 Thi use and ejection ratio characteristics at university in the stream velocities		
Velocity [m/s]	Thrust [N]	Ejection ratio	
1m/s	21.03	7.732	
10m/s	17.86	5.167	
30m/s	14.874	3.113	

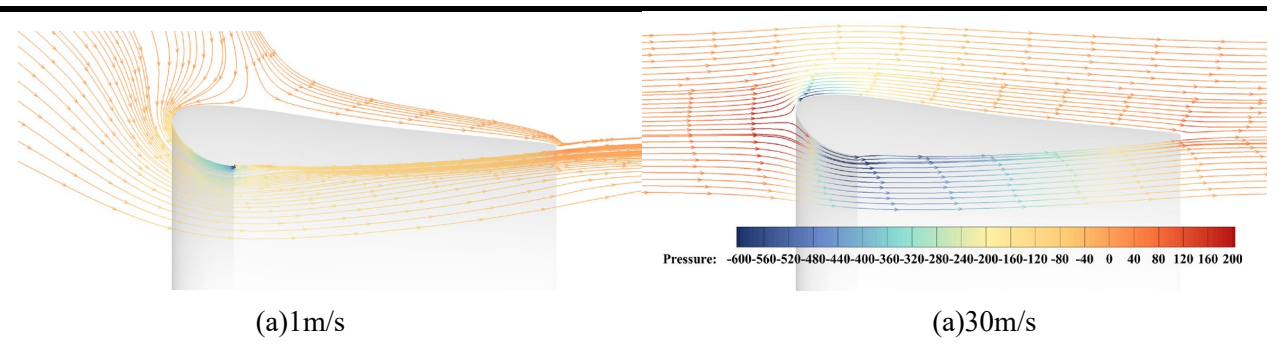


Fig. 13 Comparison of cross-sectional streamlines at 1m/s and 30m/s

Length of bladeless duct

Similar to traditional ducted fans, the length of the duct may affect the propulsion performance of the bladeless duct. This section studies the influence of the duct length on the thrust and ejection characteristics based on configuration A. When the duct length is changed, the outlet area is kept constant. The model

comparison of the three configurations studied is shown in Fig. 14.

Table 8 shows the effect of duct length on the thrust and ejection ratio characteristics of bladeless duct. As the duct length decreases, the thrust gradually increases, which is mainly affected by two aspects. The first aspect is that the shortening of the duct length increases the negative pressure peak at the lip, and the second aspect is that the increase in the expansion slope of the outer wall leads to the increase in the high pressure at the trailing edge of the outer wall. These two factors lead to better thrust characteristics. As the duct length decreases, the required power also decreases, and the propulsion efficiency increases. As the duct length decreases, the expansion slope of the inner wall increases, in the absence of a jet, while the mass flow rate through the duct section is larger in the presence of a jet, thus achieving a higher ejection ratio.

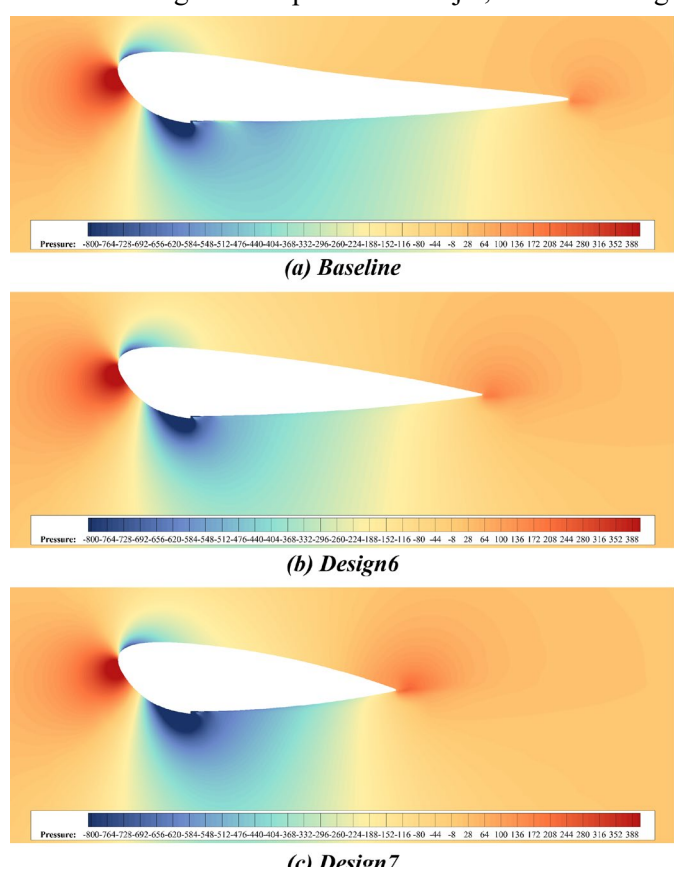


Fig. 14 Cross-sectional pressure distribution of flow field with different duct length configurations

Table 8 Thrust and ejection ratio characteristics of different duct length configurations

Configuration	Thrust[N]	Power[W]	Ejection ratio
Baseline	14.874	991.77	3.113
design6	15.83	925.0	4.40
design7	16.3	866.1	5.06

Ground Principle Test Verification of Bladeless Propulsion Fan

Ground test principle verification is not only an important way to test numerical simulation methods, but also an effective means to explore the performance of ejection power fans, which is of great significance for the next step of work. The bladeless duct was made by 3D printing. It was scaled down from the configuration A mentioned above. The smallest diameter of the inner wall is about 107mm. There are four air inlets on the outer surface. It is connected to the compressor through four air pipelines. The compressor It can nominally output a mass flow rate of 0.034kg/s. Since the fan is connected to the compressor through a hard pipeline, the thrust generated by the fan cannot be accurately measured and can only be used as a qualitative principle verification flow spectrum test. It can be proved that the effect of backward acceleration of airflow induced by low pressure inside the duct is quite significant. You can even see that the airflow that has flowed through the lips can still be sucked in.



Fig. 15 Ground Principle Verification Flow Spectrum Test

Summary

This paper takes the bladeless ducted propulsion system as the research object, we derives the theoretical expression of the thrust and power characteristics based on momentum theory. Then, the numerical simulation method of the bladeless power duct is studied. Based on the RANS method, the influence of model complexity and grids amounts on propulsion characteristics is studied, and the difference between three-dimensional configuration and two-dimensional configuration are studied; then the influence of several important design variables on the propulsion performance of the bladeless power duct and its flow mechanism are studied. Finally, the ground principle flow spectrum test of the bladeless ducted propulsion system is verified, and the suction effect of the fan is verified. The following conclusions are formed:

- 1) The theoretical expression of thrust and power characteristics of the bladeless ducted propulsion system based on momentum theory are modified from the traditional duct fan momentum theory, and mainly consider the influence of the inner jet on the thrust characteristics and power characteristics. The power characteristic calculation method can be calculated from the kinetic energy change rate and enthalpy change rate from the duct component view and the compressor component view.
- 2) As a relatively new form of thrust, bladeless ducted propulsion system may have different degrees of model simplification methods. This paper comprehensively considers the computational cost and computational efficiency, and selects a model that does not consider the internal flow channel for subsequent comparative research; and compares the performance of grids with different sparsity levels, and selects 3.2 million grids as the baseline; in the comparison of three-dimensional and two-dimensional flow fields, the three-dimensional flow field has a higher suction dimension, so the two show flow field information with similar shapes but different specific values.

- 3) Some conceptual design parameters of bladeless power duct have a great influence on the performance of bladeless duct. The duct outlet area and length have an important influence on the ejection ratio of the bladeless duct. Within the research range, the ejection ratio increases monotonically with the increase of the duct outlet area, and the maximum ejection ratio exceeds 15.6. At the same time, the duct outlet area and length also has a certain influence on the thrust; similar to the characteristics of traditional ducted fans, under the same mass flow rate of the jet, the incoming flow velocity has a more obvious effect on the flow characteristics of the duct outlet and the thrust level of the duct;
- 4) This paper conducts ground principle verification of the bladeless duct propulsion system. By placing a smoke source in front of the duct, the suction effect of the bladeless power duct can be observed. The current ground test verification does not measure the thrust and power, which will be studied in the future.

Copyright Statement

The authors confirm that they, and/or their company or organization, hold copyright on all of the original material included in this paper. The authors also confirm that they have obtained permission, from the copyright holder of any third party material included in this paper, to publish it as part of their paper. The authors confirm that they give permission, or have obtained permission from the copyright holder of this paper, for the publication and distribution of this paper as part of the ICAS proceedings or as individual off-prints from the proceedings.

Reference

- [1] Fei Zhao. The Design and Research of Bladeless Fan and Its Internal Mini-fan [D]. Zhejiang University, 2014.
- [2] https://www.jetoptera.com/
- [3] Guiling Fang. The Present Status and Prospect of Bladeless Fan [J]. ELECTRICAL APPLIANCES, 2020(09):56-58.
- [4] Wei Zhang. A brief discussion on the principle and application of bladeless fans and their industrial prospects [J].Guide to business,2012(04):285.DOI:10.19354/j.cnki.42-1616/f.2012.04.204.
- [5] L. Blain, "Jetoptera targets Mach 0.8 with bladeless-propulsion VTOL aircraft," New Atlas (2023).
- [6] P. Miller, "Dyson's air multiplier is the overpriced bladeless fan you never asked for," Endgate (2009).
- [7] Kashif Mehmood, Aamer Shahzad, Muhammad Nafees Mumtaz Qadri. Flow physics of annular and semi-annular fanjet and integration scheme with aircraft wing [J]. Physics of Fluids, 2023, 35. 10.1063/5.0165058.
- [8] Ang, Li, Jun Chen, Jun Chen. Influence of Geometric Parameters on Aerodynamic and Acoustic Performances of Bladeless Fans [C]. ASME-JSME-KSME 2019 8th Joint Fluids Engineering Conference. 2019-5220.
- [9] Hong Li. Experimental research and numerical analyze on the outlet annular slot jet of the bladeless fan [D]. Zhejiang Sci-Tech University,2018.
- [10] Guangxing Zhang. Study on External Performance and Internal Flow Field of Vaneless Fan [D]. Zhejiang Sci-Tech University,2013.
- [11] Yu Wang. Investigation on the Optimization of Bladeless Fan in Performance of Air Supply [D]. Huazhong University of Science and Technology,2019.

[12] Lei Wang. Research on air-assisted spray system based on annular jet technology [D]. Southwest University,2022.DOI:10.27684/d.cnki.gxndx.2021.000510.